jove

Biofunctionalization of Magnetic Nanomaterials

Nouf A. Alsharif[1], **Jasmeen S. Merzaban**[2], **Jürgen Kosel**[1,2]

[1] Division of Biological and Environmental Sciences and Engineering, King Abdullah University of Science and Technology [2] Division of Computer, Electrical and Mathematical Sciences and Engineering, King Abdullah University of Science and Technology

Corresponding Author

Nouf A. Alsharif

nouf.alsharif@kaust.edu.sa

Citation

Alsharif, N.A., Merzaban, J.S., Kosel, J. Biofunctionalization of Magnetic Nanomaterials. *J. Vis. Exp.* (161), e61360, doi:10.3791/61360 (2020).

Date Published

July 16, 2020

DOI

10.3791/61360

URL

jove.com/video/61360

Abstract

Magnetic nanomaterials have received great attention in different biomedical applications. Biofunctionalizing these nanomaterials with specific targeting agents is a crucial aspect to enhance their efficacy in diagnostics and treatments while minimizing the side effects. The benefit of magnetic nanomaterials compared to non-magnetic ones is their ability to respond to magnetic fields in a contact-free manner and over large distances. This allows to guide or accumulate them, while they can also be monitored. Recently, magnetic nanowires (NWs) with unique features were developed for biomedical applications. The large magnetic moment of these NWs enables a more efficient remote control of their movement by a magnetic field. This has been utilized with great success in cancer treatment, drug delivery, cell tracing, stem cell differentiation or magnetic resonance imaging. In addition, the NW fabrication by template-assisted electrochemical deposition provides a versatile method with tight control over the NW properties. Especially iron NWs and iron-iron oxide (core-shell) NWs are suitable for biomedical applications, due to their high magnetization and low toxicity.

In this work, we provide a method to biofunctionalize iron/iron oxide NWs with specific antibodies directed against a specific cell surface marker that is overexpressed in a large number of cancer cells. Since the method utilizes the properties of the iron oxide surface, it is also applicable to superparamagnetic iron oxide nanoparticles. The NWs are first coated with 3-aminopropyl-tri-ethoxy-silane (APTES) acting as a linker, which the antibodies are covalently attached to. The APTES coating and the antibody biofunctionalization are proven by electron energy loss spectroscopy (EELS) and zeta potential measurements. In addition, the antigenicity of the antibodies on the NWs is tested by using immunoprecipitation and western blot. The specific targeting of the biofunctionalized NWs and their biocompatibility are studied by confocal microscopy and a cell viability assay.

Introduction

A unique property of magnetic nanomaterials is their ability to respond to magnetic fields[1], which can be beneficially utilized to actuate them in many ways , while they can also be monitored, for instance, by magnetic resonance imaging (MRI). When applying an alternating magnetic field at high frequency, they can generate heat, which can induce hyperthermia, providing a therapeutic option[1]. Another approach is photothermal treatment, which can be realized with a near infrared (NIR) laser[2,3].

Among the large number of magnetic nanomaterials, iron oxide has received the greatest attention in biological applications such as magnetic separation, hyperthermia[2,4], cell guidance[5], drug delivery[6,7,8], and as a contrast agent in MRI[9,10]. This is due to their high biocompatibility[11,12], large magnetization[11,12], ability to be coated[9,13,14,15], ability to carry drugs[2,16], ability to be functionalized with drugs[2,16] or/and targeting agents[12,13,17,18], and ability to convert optical energy to heat[2]. Recently, MagForce started in clinical trials on cancer patients using iron oxide nanoparticles for hyperthermia treatment[19].

Lately, magnetic nanowires (NWs) have been increasingly exploited for biomedical applications[3,11,16,20,21,22]. They have similar properties as magnetic nanobeads, but offer an anisotropic shape and a very large magnetic moment, which enables a very efficient remote control by a magnetic field[23,24], including low-frequency actuation to induce magneto-mechanical effects[25,26,27,28,29]. As a consequence, the NWs have been implemented for different biological applications such as exosomes isolation[30] cell tracking[21], cancer treatment[3,11,16], drug delivery[16,31,32], and as a MRI contrast agent[33].

Biofunctionalized magnetic nanomaterials with specific cell targeting ability have great potential for biomedical applications and in precision medicine[34,35]. To attach these targeting agents, a surface modification is required on the nanomaterials. Typically, they need a coating that provides a functional group, which facilitates the attachment of the treating agents. In literature, there is a large number of organic and inorganic coatings for magnetic nanomaterials. Based on the functional group that can be immobilized to the nanomaterial, these coatings can be categorized in four main groups: molecules based on carboxylic acid groups, polymers, histidine, and molecules based on silane groups.

The molecules based on carboxylic acid groups is one of the surface modification methods. It utilizes the high affinity between the negative carboxylic acid group on the coating and the positive charge on the magnetic nanomaterials[36,37,38]. The binding process of a carboxylic acid to a metal surface may involve the generation of metal-carboxylate salts or adhesion of the carboxyl group to the metal. However, for multi-segmented NWs, such as iron/gold or nickel/gold NWs, which have superb properties for bio-applications[39,40], this type of coating cannot be applied easily. It requires two different coatings at the same time: thiol groups for modifying the gold segments and carboxyl groups for magnetic segments (iron or nickel)[38]. Some examples of molecules based on carboxyl groups are hematoporphyrin, pimelic acid, palmitic acid, and 3-[(2-aminoethyl) dithio] propionic acid (AEDP)[38]. Surface modifications of magnetic nanomaterials using polymers offer some distinct advantages. Due to the large molecular weight of the polymers, it enhances the stability of the magnetic nanomaterial in a solution[38]. However, it will significantly

increase the size of the nanomaterial[38]. Polyvinylpyrrolidone (PVP), polyethyleneimine (PEI), arginine-glycine-D aspartic acid (RGD), and polyethylene glycol (PEG) are some examples of the most commonly used polymers for surface modifications. Each one has its own features and uses[38]. The third surface modification method is using a histidine coating. Histidine is a protein with a histidine amino acid side chain that has a high affinity to limited number of magnetic nanomaterials such as nickel[38]. It can be employed for protein purification processes[38,41,42]. A histidine coating can also be applied to multi-segmented NWs, such as nickel/gold NWs[38]. The silanization of a nanomaterial surface is a well-established process[38,43,44]. It is based on a silicon atom linked to any metal oxide surface through three single bonds, and at the same time this silicon atom is binding to the functional group at the end through an alkyl chain[38,43,44]. The advantage of this coating is providing free amine groups, and it has the ability to coat both magnetic and non-magnetic materials[38,45], such as nickel and gold, respectively. Therefore, using molecules based on the saline group is a practical route for biofunctionalizing multi-segmented NWs. Some example of molecules based on silane groups are (3-aminopropyl) triethoxysilane (APTES) and (3-aminopropyl) trimethoxysilane (APTMS)[38,45].

The addition of a targeting agent to the coating can play a significant role in both diagnosis and treatment of diseased cells, and, at the same time, minimize the side effects on healthy tissues[46,47]. The addition of a targeting agent on the surface of nanomaterials enhances both cellular selective binding and internalization through endocytosis receptors[7]. Without these targeting ligands, nanomaterials interact nonspecifically with cell membranes, which binds at a lower rate compared to the nanomaterials with the ligands[48]. One of the challenges of targeting cancer tissues is their characteristic similarity to healthy tissues. Therefore, the success of targeting depends mainly on determining the appropriate ligand to use as a biological target[49,50]. Various targeting agents have been employed to direct nanomaterials to cancer cells[48,51] (e.g., CD44, due to its high expression in cancer cells compared to healthy cells[52,53,54,55]).

Targeting agents can be categorized into three main groups, based on the components they are made of and their complexity: aptamer-based targeting, ligand-based targeting, and antibody-based targeting. Aptamers are short chemically synthesized strands of DNA or RNA-oligonucleotides that are folded into two- and three-dimensional structures, making them capable of targeting a specific antigen, most often proteins[56]. Ligand-based targeting includes peptides and short amino acid chains[57]. Antibody-based targeting involves the use of a whole antibody, or antibody fragments, such as single-chain variable fragments or antigen-binding fragments[51]. Using this method has the advantage of possessing two binding sites with a high binding affinity to its specific target antigen, which gives it an exceedingly high selectivity[58]. The binding sites are analogous to a lock and the antigen to a key[58].

In this work, the NWs used were fabricated by electrodeposition onto aluminum oxide membranes, a method described in detail in a previous publication[59]. The focus here, is on releasing these iron-iron oxide (core-shell) NWs from the membranes and biofunctionalizing them with specific antibodies to provide a targeting ability. The antibodies cannot bind directly to the iron-iron oxide NWs and require a linker. Coating the NWs with APTES provides free amine groups, enabling the covalent attachment via the carboxyl group on the antibodies (**Figure 1**). The advantage of the APTES coating is its ability to work for both magnetic[21]

and non-magnetic[60] materials, such as iron/gold or nickel/gold NWs[45]. All the coating and biofunctionalization steps explained in this protocol can be utilized with any iron/iron oxide nanomaterial, in general. Iron/iron oxide NWs were used here as an example. The results show that the antibody-functionalized NWs have a high antigenicity to specific cell surface receptors, which can be used for different applications. Examples include cell separation, drug delivery, specific cancer cell treatment using photothermal and/or magneto-mechanical treatments.

Protocol

CAUTION: Always consult all relevant material safety data sheets (MSDS) before use. Use all appropriate safety practices and personal protective equipment (safety glasses, gloves, lab coat, full length pants, closed-toe shoes). Perform all biological reactions in the biological fume hood.

NOTE: This protocol is intended to produce 2 x 10^{10} biofunctionalized NWs/mL equivalent to 0.36 mg of iron/mL coated with anti-CD44 antibodies with a density of 3 x 10^4 antibodies/NW. The iron-iron oxide (core-shell) NWs are 2.5 µm long and have a diameter of 41.5 nm.

1. Release of iron nanowires

NOTE: The fabrication process of the iron/iron oxide NWs was explained in detail in a previous publication[59].

1. On a cutting mat, cut the aluminum (Al) discs (**Figure 2A**) into small pieces (**Figure 2B**) using a single edge blade and a small hammer to fit into a 2 mL tube. Use tweezers to transfer the small Al pieces to the tube.
2. Fill the 2 mL tube, containing the small Al pieces, with 1 mL of 1 M sodium hydroxide (NaOH). Make sure all the Al pieces are covered with the NaOH.
3. Leave the solution working for 30 min at room temperature inside of a chemical fume hood.
4. Remove only the Al pieces using the tweezer and keep the released NWs (black clusters, **Figure 3A**) in the NaOH solution for an additional 30 min. Do not change the NaOH solution.
5. Collect the NWs by placing the 2 mL tube in a magnetic rack and wait for 2 min before removing the old 1 M NaOH solution. Replace it with fresh NaOH solution.
6. Sonicate the 2 mL tube containing the NWs for 30 s and leave it for 1 h inside a chemical fume hood.
7. Repeat steps 1.5-1.6 at least four times.
8. Wash the NWs by placing the 2 mL tube in the magnetic rack and wait for 2 min.
9. Discard the NaOH solution and replace it with 1 mL of absolute ethanol.
10. Sonicate the tube for 30 s.
11. Place the 2 mL tube in the magnetic rack and wait 2 min.
12. Discard the old absolute ethanol solution and replace it with 1 mL of fresh absolute ethanol and sonicate for 30 s.
13. Repeat step 1.11 and 1.12 for at least four times.
14. Keep the NWs in 1 mL of absolute ethanol at room temperature until they are needed.
15. Measure the concentration of iron and hence the NWs by using inductively coupled plasma mass spectrometry (ICP-MS).

    NOTE: The protocol can be paused here. However, for long-time storage, do not release the NWs from the

Al template until needed. Keeping the released NWs precipitating in the ethanol for a long time without frequent sonication will create aggregations that will need longer times of sonication to be separated.

2. Coating the nanowires with APTES

NOTE: In this protocol, 100 µL of APTES solution (density of 0.946 g/mL[61]) is enough to coat 1.6 x 10^7 m^2/g of NWs. If there is a change in the ratio or the mass of the nanomaterial, the APTES volume should be adjusted accordingly.

1. Transfer the NWs from step 1.14 to a 5 mL glass tube using a 1 mL pipette.
2. To collect any NWs left in the 2 mL tube, wash the empty 2 mL tube twice by adding 1 mL of absolute ethanol and transfer it to the 5 mL glass tube using a 1 mL pipette.
3. By using the pipette, take 100 µL of APTES and add it to the NW solution directly.
4. Vortex the 5 mL glass tube for 10 s.
5. Adjust the 5 mL glass tube on the clamp of a laboratory retort stand.
6. Place half of the 5 mL glass tube inside of the water of the ultrasonic bath and sonicate for 1 h.
7. Take out the 5 mL glass tube from the ultrasonic bath and add 400 µL of deionized (DI) water followed by 20 µL of 1 M NaOH (basic catalysis).
   CAUTION: It is important to add the DI water first.
8. Adjust the 5 mL glass tube, as explained in steps 2.5-2.6, and sonicate for another 1 h.
9. Take out the 5 mL glass tube from the ultrasonic bath.
10. Place a magnet next to the glass tube for 5 min to collect the NWs.
11. Replace the supernatant with 1 mL of fresh absolute ethanol and sonicate for 10 s.
12. Repeat steps 2.10-2.11 four times.
13. Transfer all NWs suspended ethanol to a new 5 mL glass tube using a 1 mL pipette.
    NOTE: The APTES coated NWs can be stored in a glass tube with ethanol until they are needed. The protocol can be paused here.

3. Biofunctionalization of the nanowires

1. Activating the antibodies
   NOTE: To achieve approximately 3 x 10^4 parts of antibody/NW, use 30 µL of antibody (1 mg/mL) per 0.1 mg of iron.
   1. In a 2 mL tube, dissolve 0.4 mg of 3-3-dimethyl-aminopropyl carbodiimide (EDC) and 1.1 mg of sulfo-N-hydroxysulfosuccinimide (Sulfo-NHS) in 1 mL of 2-N-morpholino ethanesulfonic acid hydrate (MES) (pH 4.7).
      NOTE: The EDC/sulfo-NHS mixture should be fresh and prepared before using.
   2. In a new 2 mL tube, add 30 µL of anti-CD44 antibody (1 mg/mL), 960 µL of 0.1 M of phosphate buffered saline (PBS, pH 7), and 10 µL of EDC/sulfo-NHS mixture (prepared in step 3.1.1), respectively.
   3. Place the 2 mL tube in a tube shaker at 10 x *g* for 15 min at room temperature.
2. Preparation of the APTES coated nanowires
   1. During the 15 min incubation in step 3.1.3, wash the NWs by placing a magnet next to the APTES coated NWs tube (from step 2.13) for 2 min to collect the NWs.

2. Discard the ethanol and replace it with 1 mL of 0.1 M PBS (pH 7), and then sonicate for 10 s.
3. Repeat step 3.2.1-3.2.2 four times.
4. Collect the NWs, as explained in step 3.2.1, and discard the 0.1 M PBS. Keep the NWs in the tube without any solution.

3. Attachment of the antibodies
    1. Transfer all the activated antibody solution (prepared in step 3.1.3) to the NWs tube (prepared in 3.2.4) and sonicate for 10 s.
    2. Place the glass tube in the rotator overnight at 4 °C.
    3. Collect the NWs using a magnet as in step 3.2.1 and discard the supernatant.
    4. Adding 1 mL of 2% bovine serum albumin (BSA) solution for 1 h at 4 °C to block the reaction.
    5. Check the antigenicity of the antibody functionalized NWs, for example, using immunoprecipitation (IP) and western blot (WB) assays.
    NOTE: For better results, use the biofunctionalized NWs in the IP, WB, or biocompatibility assay immediately after the blocking step.

4. Biocompatibility assay

NOTE: To study the biocompatibility of the NWs, various cell viability assays and different cell lines can be employed. The concentration of the NWs used here is based on a previous publication[16]. The cell seeding should be done one day before the NW biofunctionalization.

CAUTION: All the below steps should be done under the biosafety cabinet.

1. In a 96-well plate, seed nine wells with 4 x 10^4 of colon cancer cells (HCT116 cell line) suspended in McCoy's cell culture media (100 µL/well) and place it inside the incubator overnight at 37 °C and 5% carbon dioxide (CO_2).
2. Wash the NWs (from step 3.3.4) with PBS by collecting them using a magnet as in step 3.2.1 and replace the old solution with 1 mL of 0.01 M PBS (pH 7). Repeat this step three times.
3. Wash the NWs (from step 4.2) with warmed McCoy's media by collecting them using a magnet as in step 3.2.1 and replace the old PBS with 1 mL of warmed McCoy's media. Repeat this step three times.
4. Collecting the NWs (from step 4.3) using a magnet as in step 3.2.1 and replace the 1 mL of warmed McCoy's media with 900 µL of warmed McCoy's media. The NWs concentration should be 0.02 mg of NWs per mL.
5. Take the 96-well plate (from step 4.1) from the incubator to the biosafety cabinet.
6. Under the biosafety cabinet, discard the old media from the cells and replace it with 100 µL of suspended NWs (prepared in step 4.4).
7. Shake the plate (prepared in step 4.6) by hand and then incubate it for 24 h inside the incubator at 37 °C and 5% CO_2.
8. The next day, take out the 96-well plate (prepared in step 4.7) from the incubator. Under the biosafety cabinet, add 11 µL of the cell viability reagent (**Table of Materials**) to each well using the multiwall pipette.
9. Shake the plate with the plate shaker at a speed of 10 x *g* for 10 s.
10. Incubate the plate for 1 h in the incubator.

11. Take out the 96-well plate (prepared in step 4.10) from the incubator. Read the plate in the microplate reader (**Table of Materials**) by measuring the absorbance of the cell viability reagent (excitation 540 nm, emission 590 nm).

Representative Results

It is important to cut the aluminum (Al) discs (**Figure 2A**) into small pieces (**Figure 2B**) to fit in the tube used. After adding 1 M NaOH to the Al pieces, a reaction should start immediately, which is observed by the creation of bubbles. If no reaction occurs in 1 min or if the reaction is very fast and the solution turns completely turbid with a white cloud, remove the old NaOH solution immediately and replace it with a fresh solution. Check the pH value of the NaOH solution. It should be pH>12. When the NWs are released from the Al pieces in the first 30 min with NaOH, the NWs (black clusters, **Figure 3A**) will be floating within the NaOH solution. In the last step of releasing the NWs, the solution should be homogeneous. No cluster of NWs should be there (**Figure 3B**). If NWs were collected with a magnet for 3 min, the solution should be clear, and the NW pellet should be black (**Figure 3C**). If the pellet was gray, discard the tube and start again with a new Al sample.

During the releasing process, the NWs obtain a native iron oxide layer with around 5 nm thickness, which is similar to previous reports[11,16,20]. This oxide layer has an important contribution to the biocompatibility[16], functionalization[16,18] and magnetic properties[20] of the NWs. However, keeping the NWs in their template (i.e., not releasing them) until needed will prevent them from any environmental effects on them. The average diameter and length of the NWs after the releasing process were 2.5 µm and 41.5 nm, respectively. The mass of a single NW can be calculated as explain in **Table 1** and it confirmed by inductively coupled plasma mass spectroscopy (ICP-MS). Here, each alumina disc contained around 0.3 mg of iron.

To reduce the aggregation of the NWs after releasing and enable further functionalization, the NWs were coated with APTES. This coating provides free amine groups and has the ability to coat both magnetic and non-magnetic materials[39,45], making it suitable for coating multi-segmented NWs such as iron/gold NWs. During the nanowires coating, it is important to focus on two things. First, calculate the needed volume from APTES molecules[62] based on the surface area and the mass of the NWs. These calculations were presented in **Table 2**. Secondly, keep the nanowires in a continuous movement to prevent their agglomeration and the blocking of some parts of NW surfaces from APTES coating. For instance, in this protocol, the nanowires were incubated under the ultrasonic bath and rotator during the APTES coating and antibody functionalization, respectively. Each APTES molecule contains a silicon atom and a terminal functional amine group[21]. Therefore, electron energy-loss spectroscopy (EELS) maps can be used to confirm the presence of the APTES coating by showing silicon atoms (pink color) on the NW surface (**Figure 4A**). In contrast, the non-coated NWs show the iron atoms in bark blue (**Figure 4B**) and iron/oxygen mix atoms in light blue (**Figure 4B**). The corresponding EELS mapping of non-coated NWs (**Figure 4C,4D**) shows a higher intensity of iron vs. oxygen in the center (**Figure 4C**) than on the surface (**Figure 4D**), indicating an iron-iron oxide (core-shell) structure. The EELS mapping (**Figure 4C,4D**) was identified that the iron oxide layer on the NWs is Fe_3O_4 more than Fe_2O_3, which is similar to a previous publication[20].

The antigenicity of the attached antibodies can be confirmed using the IP and WB assays, where a band can be observed on the positive sample but not on the negative controls (**Figure 5**). Note that to observe a clear band, do not use less than 0.1 mg of NWs/10 x 10^6 cells. BCA assay (**Table of Materials**) in combination with some calculations presented in **Table 3** was used to quantify the antibodies number on the NW.

Furthermore, the zeta-potential measurement was used to elucidate the surface functionalization. The terminal amine group on APTES reduced the negative charge of the non-coated NWs, as shown in **Figure 6**. The antibody-functionalized NWs also changed the charge compared to the APTES-coated NWs (**Figure 6**). All the zeta-potential measurements were done at pH 7.

The specific cell targeting of the antibody-functionalized NWs can be confirmed using confocal microscopy (**Figure 7**). The biocompatibility of any new nanomaterial should be tested before starting any application. Therefore, the cell viability assay was used, and it confirmed that the non-coated, APTES coated-, and antibody coated-NWs were biocompatible even with a high concentration (**Figure 8**).

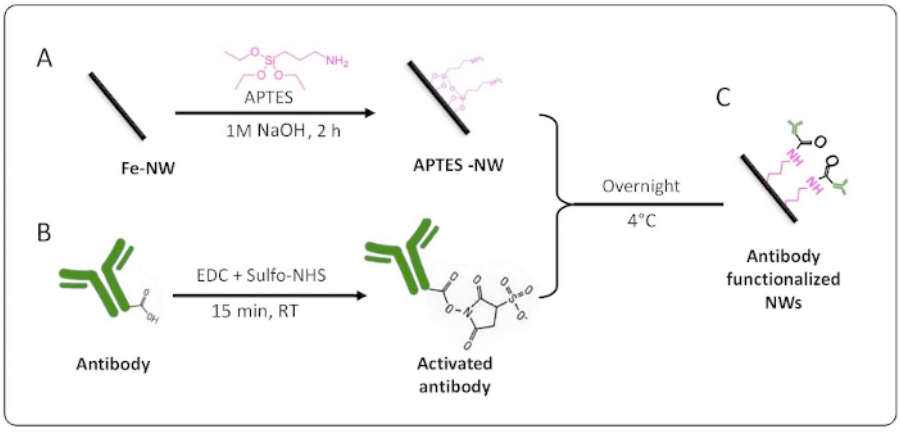

Figure 1: Schematic represents the coating and biofunctionalization method of the nanowires. (**A**) Coating iron NWs with APTES. (**B**) Activating the antibodies by using EDC + Sulfo-NHS, to have at the end (**C**) an antibody functionalized nanowire. Please click here to view a larger version of this figure.

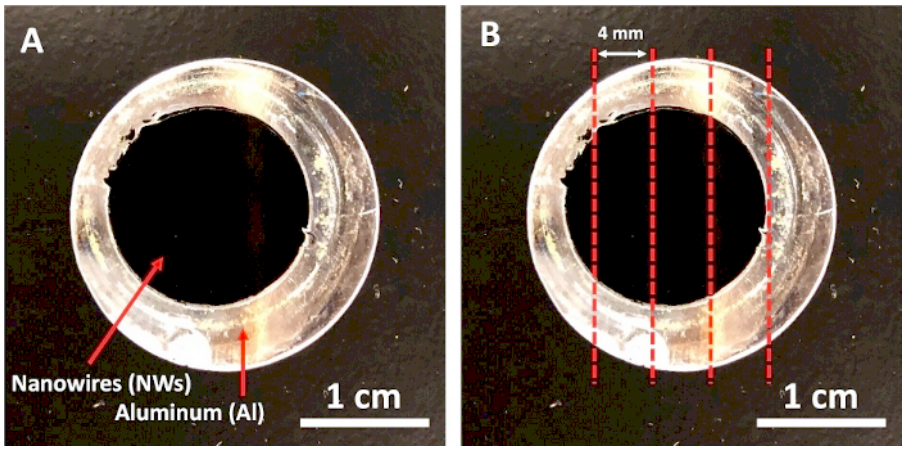

Figure 2: Iron deposited aluminum disc. (**A**) The aluminum disc before the cutting. (**B**) The red lines showed where to cut the disc. Please click here to view a larger version of this figure.

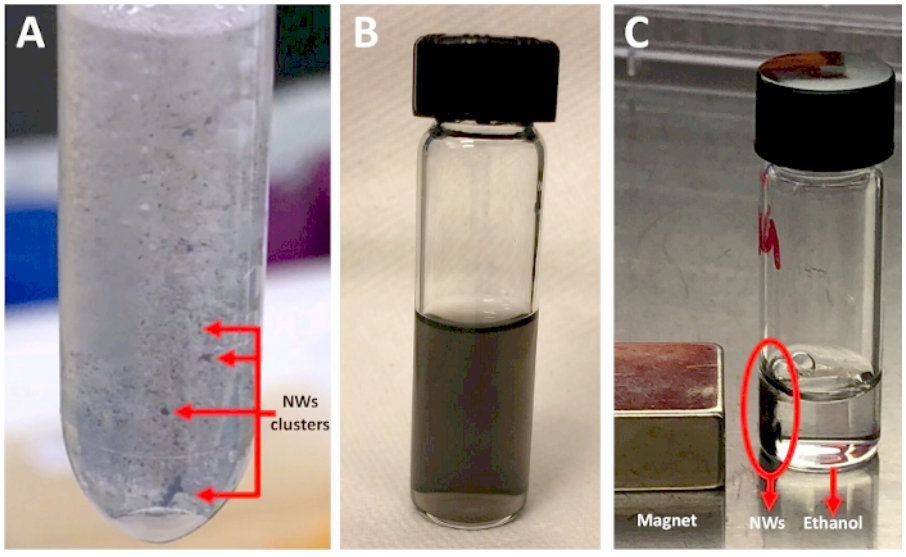

Figure 3: Nanowire release steps. (**A**) Clusters of nanowires are floating in NaOH solution. The image was taken 10 min after adding the NaOH and after removing the Al membrane. (**B**) Nanowires suspended in ethanol. The photo was taken in the last releasing step, immediately after the sonication step. (**C**) Black nanowire pellet collected by a magnet. Please click here to view a larger version of this figure.

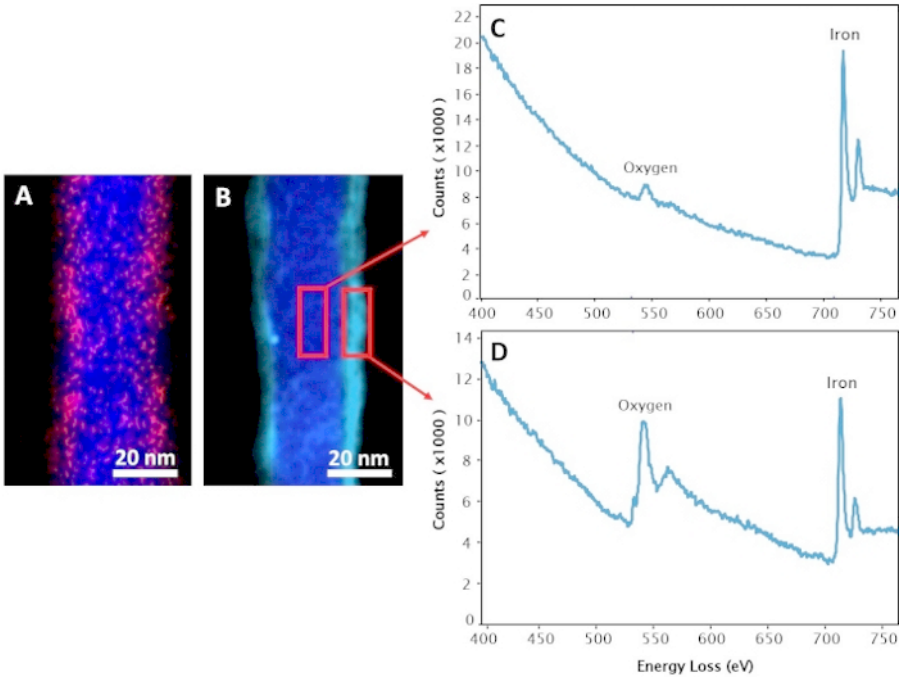

Figure 4: Electron energy-loss spectroscopy (EELS) map. (**A**) APTES coated nanowire (APTES-NW). The blue and pink colors represent iron and silicon atoms, respectively. (**B**) Non-coated nanowire (NW). The bark blue and light blue colors represent the iron and iron/oxygen mix mapping, respectively. The corresponding EELS mapping of (**C**) the core and (**D**) the shell of the non-coated NWs. Please click here to view a larger version of this figure.

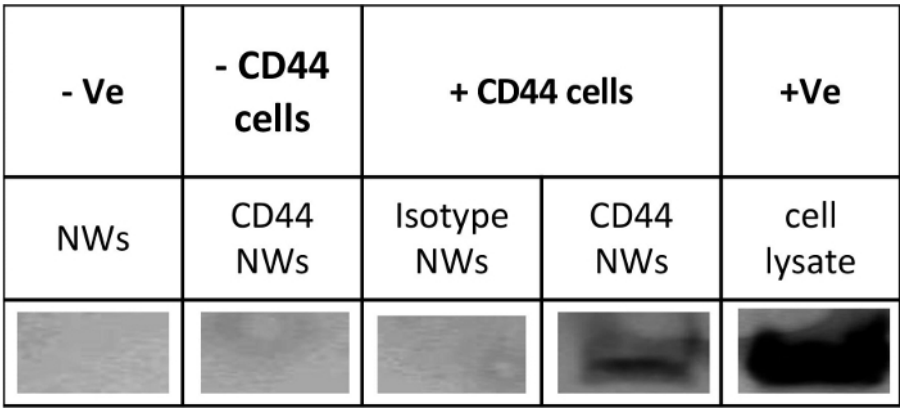

Figure 5: Confirmation of functionalization and activity of antibody conjugated nanowires. The antigenicity of CD44-NWs was confirmed by using immunoprecipitation (IP) and western blot (WB). +Ve: represents the positive control (full cell lysate). -Ve: represents the negative control (only non-coated NW). – CD44 cells: represents cells that do not express CD44 antigen; + CD44 cells: represents colon cancer cells that express CD44 antigen. This is a representative blot of n = 3 independent experiments. Please click here to view a larger version of this figure.

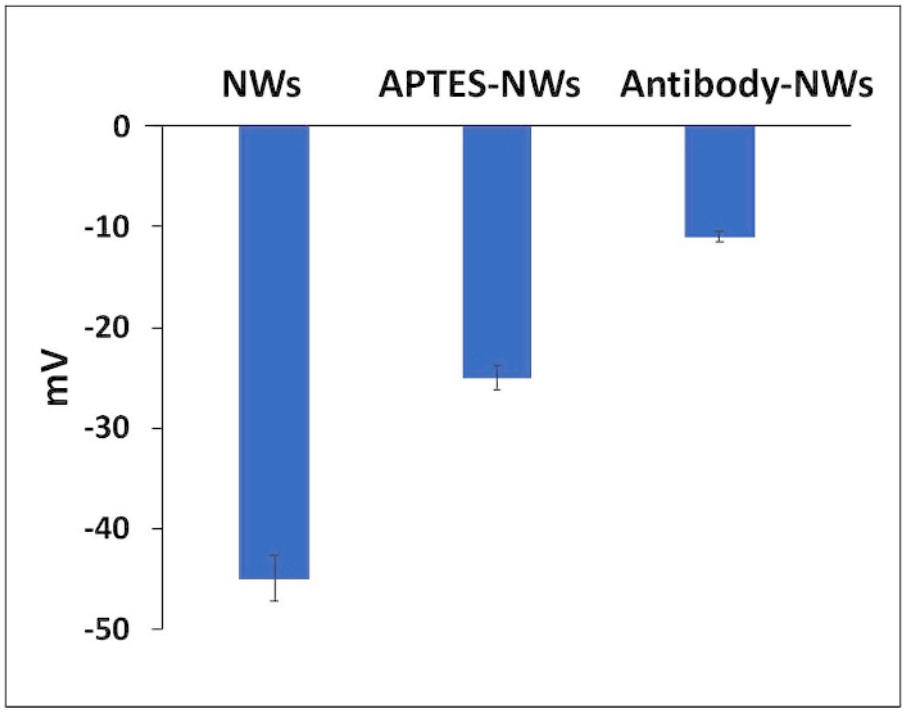

Figure 6: Zeta potential values for NWs, APTES-NWs, and antibody. The bars represent the mean ± standard error.

Please click here to view a larger version of this figure.

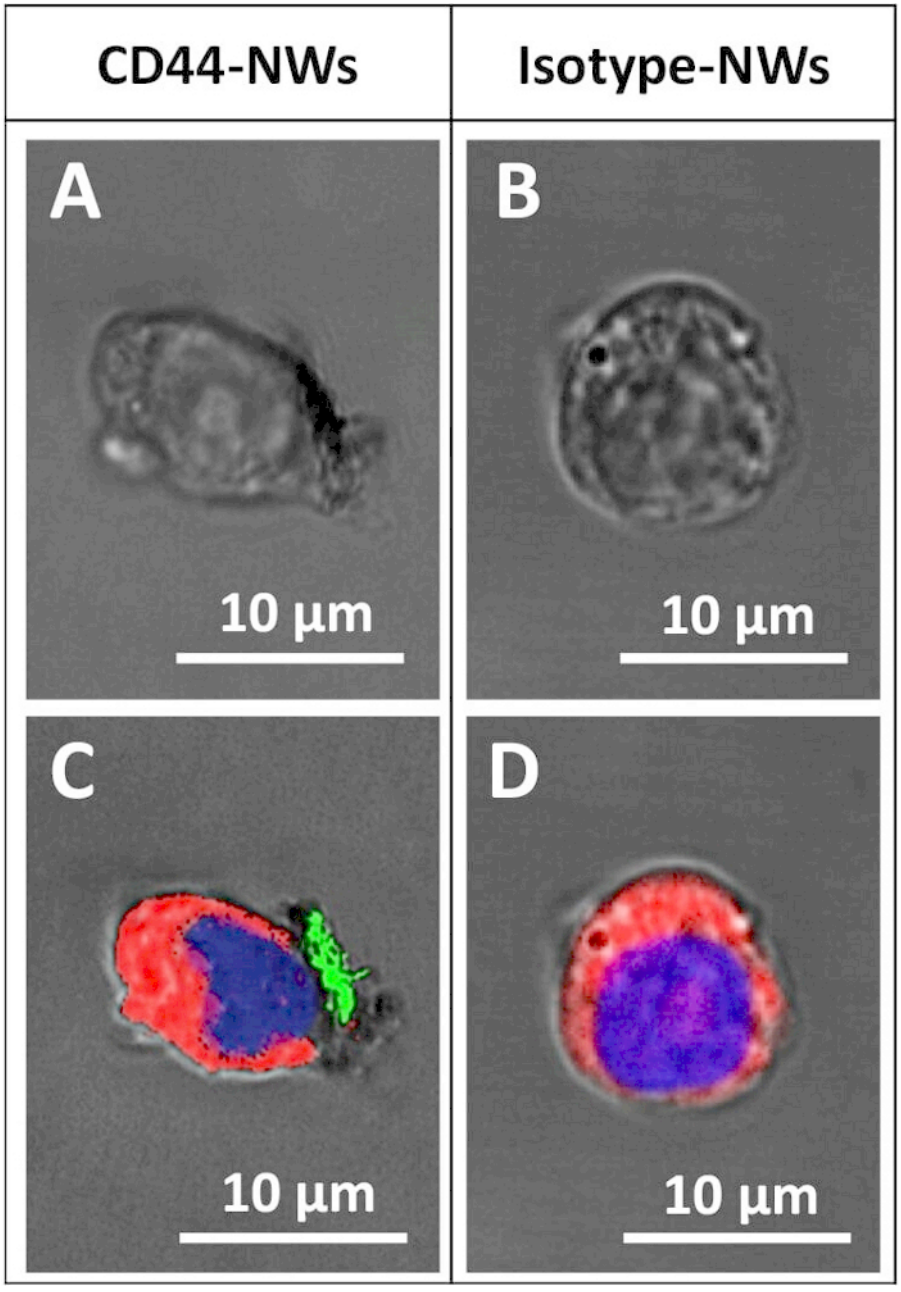

Figure 7: Confocal microscopic images shows the specific targeting. CD44-NWs are shown attaching (**A** and **C**), while the Isotype-NWs (negative control) did not attach (**B** and **D**). The red, blue, and green colors represent the cell membrane, nucleus, and cluster of CD44-NWs, respectively. A and B are the bright field images of C and D, respectively. Please click here to view a larger version of this figure.

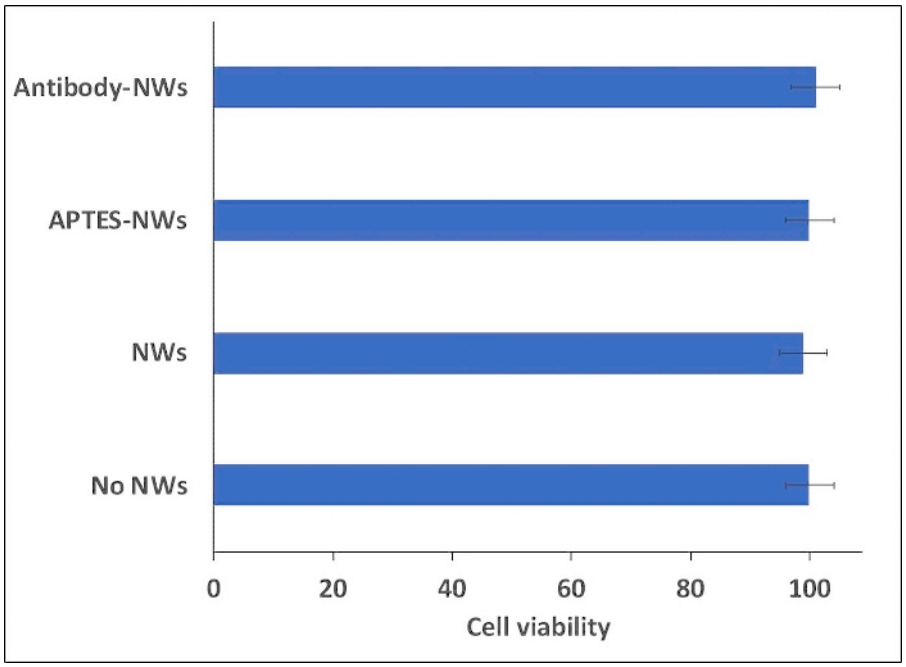

Figure 8: Cell viability study of colon cancer cells (HCT116) incubated with different formulations of nanowires. The cells were treated with NWs after 24h of incubation and then incubated for 24h with the NWs. All the experiments were carried out inside an incubator at 37 °C. The bars represent the mean ± standard error. Please click here to view a larger version of this figure.

Parameter	Value	Unit		
Length of Fe NW (h)	2.6	µm		
Radius (diameter/2) (r)	0.01679231	µm		
Fe density (D)	7.87	g/cm^3		
1 Fe NW volume (V)= π r^2h	2.30E-15	cm^3		
1 Fe NW mass = V x D	1.80E-08	µg		
1 Fe NW surface area = 2π r^2 + 2πrh	2.76E-01	$µm^2$	2.8E+05	nm^2

Table 1: Calculation of the iron NW mass.

Parameter	Value	Unit
Density of APTES/100 µL*	9.50E-01	g
Moleculer wight (MW) of APTES	2.21E+02	g/mol
Number of APTES mole = mass/MW	4.29E-03	mol
Number of APTES molecules/100 µL**	2.57E+21	molecules
APTES size ***	5.00E-01	nm
APTES surface area	2.00E-01	nm^2
NW surface area******	2.76E+05	nm^2
Number of NWs in 0.3mg of NW ******	1.70E+10	NWs
Number of APTES molecules needed to creat one layer around the NW	1.38E+06	APTES molecule
Number of APTES molecules needed for 0.3 mg of NWs	2.35E+16	APTES molecule
*Refrence number 61		
** Number of molecules = Number of mol*avogadro number (6E+23)		
***Refrence number 62		
****From Table 1		

Table 2: Calculation the number of APTES molecules required for NWs coating.

	Y-shape IgG antibody	NW
Mass for one antibody	2.3E-13 µg	1.8E-08 µg*
Surface area for one antibody	23 nm^2	2.6E+05 nm^2
Based on BCA assay	0.3 mg per 1 mg	
The number of the antibody molecule and NW in 0.3 mg of antibody per mg of NW	~1E+15 antibodies ** per ~5.6E+10 NWs	
Number of antibody molecule per NW	~2E+04 antibodies per 1 NW***	
*Calculated from table 1		
**The number of the antibodies in 0.3 mg was calculated by dividing the antibody number that we received from the BSA assay (0.3 mg) by the average molecular weight of Y-shaped IgG antibodies (180 kDa = 3E-16 mg).		
***Based on the surface area of one molecule of Y-shaped IgG antibodies (~23 nm2) and the surface area of one NW (~2.6E+05 nm2), around 1E+04 antibodies would be enough to create a monolayer on the NW. In our case, the density of antibody was two times more than the expected amount. This can be related to the APTES coating that provides more arms that allows the high attachment of the antibodies. This case ensures that the NW is fully covered with the antibodies and the opportunity for the antibody to bind to a cell surface antigen, regardless of the orientation of the NWs will be high. However, if the antibody density is lower than the expected number (1E+04 molecule of antibody), then the binding chance between the cell and the NWs will be lower.		

Table 3: Calculation of the number of antibodies on the nanowire.

Discussion

As with any nanomaterial fabrication and coating method, a high quality of the solutions used is required. The release (1 M NaOH) and functionalization (MES) solutions can be reused several times. However, checking their pH value before starting a new process is very important. In the release step, washing the NWs with NaOH should be carried out at least four times. The better the washing, the better the stability of the NWs and the less they are aggregate. The oxide layer enhances the stability of the NWs upon immersion in ethanol or water[63] .

The diameter and the length of the NWs were affected after coating them with APTES and antibodies. Here, the diameter increased from 41.5 nm to 70 nm, and the length decreased from 2.5 µm to 1.6 µm, due to the sonication steps that break the NWs. Therefore, it is essential characterize the morphology of the NWs after the biofunctionalization step.

The attachment of the antibodies to the NWs relies on the covalent interaction between the amine group (on APTES) and the carboxyl group (on the antibody). Therefore, confirming the presence of the APTES coating is an important step, for which we used EELS mapping. The coating

method is safe and straightforward. It does not need high temperatures or long incubation times. Also, APTES coating works as a linker to enable the covalent attachment of other antibodies or proteins that has a carboxyl group.

In the case of biofunctionalizing the NWs with an antibody, the antigenicity of the antibodies' binding sites after the biofunctionalization process can be affected. The IP and WB method can be used to investigate this issue. Using the biofunctionalization method mentioned in this protocol will allow the antibodies to bind to the NWs with high antigenicity to a specific cell receptor. Moreover, biofunctionalizing the NWs with antibodies added the ability to target the cells with the receptor of interest, CD44 here. This was confirmed by confocal microscopy. Although the biocompatibility of the uncoated NWs was high (>95%), adding APTES coating or antibodies to the NWs enhanced their biocompatibility 100%.

Further, the coating and biofunctionalization protocol is efficient, economical, and reproducible. It should be applicable to any other iron-iron oxide nanomaterial, whereby the concentration of both the coating and the attached antibodies should be optimized based on the surface area and the mass of the nanomaterial. This protocol can be done safely at ambient conditions in the general laboratory. The biofunctionalization has significantly enhanced the biocompatibility of the nanomaterial and their targeting ability. In general, the NWs are extremely promising materials for nanomedical applications (including multi-modal or combinatorial treatments, cell detection or guidance, and biological sensing). Combined with biofunctionalization, as described here, specific cell targeting can be achieved for increased precision and efficacy.

Disclosures

The authors have nothing to disclose.

Acknowledgments

Research reported in this publication was supported by the King Abdullah University of Science and Technology (KAUST).

References

1. Dürr, S. et al. Magnetic nanoparticles for cancer therapy. *Nanotechnology Reviews.* **2** (4), 395-409 (2013).
2. Espinosa, A. et al. Duality of iron oxide nanoparticles in cancer therapy: amplification of heating efficiency by magnetic hyperthermia and photothermal bimodal treatment. *ACS Nano.* **10** (2), 2436-2446 (2016).
3. Martínez Banderas, A. I. et al. Iron-Based Core-Shell Nanowires for Combinatorial Drug Delivery, Photothermal and Magnetic Therapy. *ACS Applied Materials Interfaces.* (2019).
4. Das, R. et al. Tunable high aspect ratio iron oxide nanorods for enhanced hyperthermia. *The Journal of Physical Chemistry.* **120** (18), 10086-10093 (2016).
5. Chen, J. et al. Guidance of stem cells to a target destination in vivo by magnetic nanoparticles in a magnetic field. *ACS Applied Materials Interfaces.* **5** (13), 5976-5985 (2013).
6. Juneja, R., Roy, I. Iron oxide-doped niosomes as drug carriers for magnetically targeted drug delivery. *International Journal of Nanomedicine.* **13**, 7 (2018).
7. Aires, A. et al. Multifunctionalized iron oxide nanoparticles for selective drug delivery to CD44-positive cancer cells. *Nanotechnology.* **27** (6), 065103 (2016).

8. Trabulo, S., Aires, A., Aicher, A., Heeschen, C., Cortajarena, A. L. Multifunctionalized iron oxide nanoparticles for selective targeting of pancreatic cancer cells. *Biochimica et Biophysica Acta -General Subjects.* **1861** (6), 1597-1605 (2017).
9. Blanco-Andujar, C. et al. Design of iron oxide-based nanoparticles for MRI and magnetic hyperthermia. *Nanomedicine.* **11** (14), 1889-1910 (2016).
10. Hachani, R. et al. Polyol synthesis, functionalisation, and biocompatibility studies of superparamagnetic iron oxide nanoparticles as potential MRI contrast agents. *Nanoscale.* **8** (6), 3278-3287 (2016).
11. Contreras, M. F., Sougrat, R., Zaher, A., Ravasi, T., Kosel, J. Non-chemotoxic induction of cancer cell death using magnetic nanowires. *International Journal of Nanomedicine.* **10** 2141 (2015).
12. Perez, J. E. et al. in *Cytotoxicity.* Ch. 12 IntechOpen, (2018).
13. Kievit, F. M., Zhang, M. Surface engineering of iron oxide nanoparticles for targeted cancer therapy. *Accounts of Chemical Research.* **44** (10), 853-862 (2011).
14. Xu, H. et al. Antibody conjugated magnetic iron oxide nanoparticles for cancer cell separation in fresh whole blood. *Journal of Biomaterials.* **32** (36), 9758-9765 (2011).
15. Zhang, L., Dong, W.F., Sun, H.B. Multifunctional superparamagnetic iron oxide nanoparticles: design, synthesis and biomedical photonic applications. *Nanoscale.* **5** (17), 7664-7684 (2013).
16. Martínez-Banderas, A. I. et al. Functionalized magnetic nanowires for chemical and magneto-mechanical induction of cancer cell death. *Scientific Reports.* **6** 35786 (2016).
17. Tian, Q. et al. Multifunctional Polypyrrole@ Fe3O4 Nanoparticles for Dual-Modal Imaging and In Vivo Photothermal Cancer Therapy. *Small.* **10** (6), 1063-1068 (2014).
18. Alsharif, N. A., Martiìnez-Banderas, A. I., Merzaban, J., Ravasi, T., Kosel, J. Biofunctionalizing Magnetic Nanowires Toward Targeting and Killing Leukemia Cancer Cells. *IEEE Transactions on Magnetics.* **2** (99), 1-5 (2018).
19. Ventola, C. L. Progress in nanomedicine: approved and investigational nanodrugs. *Journal of Pharmacy Therapeutics.* **42** (12), 742 (2017).
20. Ivanov, Y. P. et al. Tunable magnetic nanowires for biomedical and harsh environment applications. *Scientific Reports.* **6** 24189 (2016).
21. Margineanu, M. B. et al. Semi-automated quantification of living cells with internalized nanostructures. *Journal of Nanobiotechnology.* **14** (1), 4 (2016).
22. Jeon, Y. S. et al. Metallic Fe–Au Barcode Nanowires as a Simultaneous T Cell Capturing and Cytokine Sensing Platform for Immunoassay at the Single-Cell Level. *ACS Applied Materials Interfaces.* **11** (27), 23901-23908 (2019).
23. Lee, E. et al. Highly selective CD44-specific gold nanorods for photothermal ablation of tumorigenic subpopulations generated in MCF7 mammospheres. *Nanotechnology.* **23** (46), 465101 (2012).
24. Patel, N. S., Lago-Cachón, D., Mohammed, H., Moreno, J. A., Kosel, J. J. J. Iron Nanowire Fabrication by Nano-Porous Anodized Aluminum and its Characterization. *Journal of Visualized Experiments.* (152), e60111 (2019).

25. Rozhkova, E. A. et al. Ferromagnetic microdisks as carriers for biomedical applications. *Journal of Applied Physics.* **105** (7), 07B306 (2009).

26. Kim, D.H. et al. Biofunctionalized magnetic-vortex microdiscs for targeted cancer-cell destruction. *Nature Materials.* **9** (2), 165-171 (2010).

27. Kim, D.H. et al. Mechanoresponsive system based on sub-micron chitosan-functionalized ferromagnetic disks. *Journal of Materials Chemistry.* **21** (23), 8422-8426 (2011).

28. Vitol, E. A., Novosad, V., Rozhkova, E. A. Multifunctional ferromagnetic disks for modulating cell function. *IEEE Transactions on Magnetics.* **48** (11), 3269-3274 (2012).

29. Vitol, E. A., Novosad, V., Rozhkova, E. A. Microfabricated magnetic structures for future medicine: from sensors to cell actuators. *Nanomedicine.* **7** (10), 1611-1624 (2012).

30. Lim, J. et al. Direct isolation and characterization of circulating exosomes from biological samples using magnetic nanowires. *Journal of Nanobiotechnology.* **17** (1), 1-12 (2019).

31. Shore, D. et al. Electrodeposited Fe and Fe–Au nanowires as MRI contrast agents. *Chemical Communications.* **52** (85), 12634-12637 (2016).

32. Marťinez-Banderas, A. I. et al. Iron-Based Core–Shell Nanowires for Combinatorial Drug Delivery and Photothermal and Magnetic Therapy. *ACS Applied Materials Interfaces.* **11** (47), 43976-43988 (2019).

33. Martínez-Banderas, A. I. et al. Magnetic core–shell nanowires as MRI contrast agents for cell tracking. *Journal of Nanobiotechnology.* **18** (1), 1-12 (2020).

34. Zhu, L., Zhou, Z., Mao, H., Yang, L. Magnetic nanoparticles for precision oncology: theranostic magnetic iron oxide nanoparticles for image-guided and targeted cancer therapy. *Nanomedicine.* **12** (1), 73-87 (2017).

35. Guleria, A., Priyatharchini, K., Kumar, D. in *Applications of Nanomaterials.* 345-389 Elsevier, (2018).

36. Allara, D. L., Nuzzo, R. G. Spontaneously organized molecular assemblies. 2. Quantitative infrared spectroscopic determination of equilibrium structures of solution-adsorbed n-alkanoic acids on an oxidized aluminum surface. *Langmuir.* **1** (1), 52-66 (1985).

37. Allara, D. L., Nuzzo, R. G. Spontaneously organized molecular assemblies. 1. Formation, dynamics, and physical properties of n-alkanoic acids adsorbed from solution on an oxidized aluminum surface. *Langmuir.* **1** (1), 45-52 (1985).

38. Schrittwieser, S., Reichinger, D., Schotter, J. Applications, surface modification and functionalization of nickel nanorods. *Materials and Structures.* **11** (1), 45 (2018).

39. Lim, J., Choi, M., Lee, H., Kim, Y. H., Han, J. Y., Lee, E. S., Cho, Y. Direct isolation and characterization of circulating exosomes from biological samples using magnetic nanowires. *Journal of Nanobiotechnology.* **17** (1), 1 (2019).

40. Nemati, Z. et al. Magnetic Isolation of Cancer-derived Exosomes Using Fe/Au Magnetic Nanowires. *ACS Applied Nano Materials.* **3** (2), 2058-2069 (2020).

41. Hainfeld, J. F., Liu, W., Halsey, C. M., Freimuth, P., Powell, R. D. Ni–NTA–gold clusters target His-tagged proteins. *Journal of Structural Biology.* **127** (2), 185-198 (1999).

42. Agarwal, G., Naik, R. R., Stone, M. O. Immobilization of histidine-tagged proteins on nickel by electrochemical dip pen nanolithography. *Journal of the American Chemical Society.* **125** (24), 7408-7412 (2003).

43. Aswal, D., Lenfant, S., Guerin, D., Yakhmi, J., Vuillaume, D. Self assembled monolayers on silicon for molecular electronics. *Analytica Chimica Acta.* **568** (1-2), 84-108 (2006).

44. Haensch, C., Hoeppener, S., Schubert, U. S. Chemical modification of self-assembled silane based monolayers by surface reactions. *Chemical Society Reviews.* **39** (6), 2323-2334 (2010).

45. Wildt, B., Mali, P., Searson, P. C. Electrochemical template synthesis of multisegment nanowires: Fabrication and protein functionalization. *Langmuir.* **22** (25), 10528-10534 (2006).

46. Schladt, T. D., Schneider, K., Schild, H., Tremel, W. Synthesis and bio-functionalization of magnetic nanoparticles for medical diagnosis and treatment. *Dalton Transactions.* **40** (24), 6315-6343 (2011).

47. Kumar, C. S. *Magnetic nanomaterials.* John Wiley & Sons, (2009).

48. Peiris, P. et al. Precise targeting of cancer metastasis using multi-ligand nanoparticles incorporating four different ligands. *Nanoscale.* **10** (15), 6861-6871 (2018).

49. Veiseh, O., Gunn, J. W., Zhang, M. Design and fabrication of magnetic nanoparticles for targeted drug delivery and imaging. *Journal of Advanced Drug Delivery Reviews.* **62** (3), 284-304 (2010).

50. Rosenblum, D., Joshi, N., Tao, W., Karp, J. M., Peer, D. Progress and challenges towards targeted delivery of cancer therapeutics. *Nature Communications.* **9** (1), 1410 (2018).

51. Bazak, R., Houri, M., El Achy, S., Kamel, S., Refaat, T. Cancer active targeting by nanoparticles: a comprehensive review of literature. *Journal of Cancer Research Clinical Oncology.* **141** (5), 769-784 (2015).

52. Zeilstra, J. et al. CD44 expression in intestinal epithelium and colorectal cancer is independent of p53 status. *PLoS One.* **8** (8), e72849 (2013).

53. Pesarrodona, M. et al. Intracellular targeting of CD44+ cells with self-assembling, protein only nanoparticles. *International Journal of Pharmaceutics.* **473** (1-2), 286-295 (2014).

54. Chandra, V. et al. Quantitative assessment of CD44 genetic variants and cancer susceptibility in Asians: a meta-analysis. *Oncotarget.* **7** (45), 74286 (2016).

55. Thapa, R., Wilson, G. D. The importance of CD44 as a stem cell biomarker and therapeutic target in cancer. *Stem Cells International.* **2016** (2016).

56. Gao, S., Zheng, X., Jiao, B., Wang, L. Post-SELEX optimization of aptamers. *Analytical Bioanalytical Chemistry.* **408** (17), 4567-4573 (2016).

57. Das, M., Mohanty, C., Sahoo, S. K. Ligand-based targeted therapy for cancer tissue. *Expert Opinion on Drug Delivery.* **6** (3), 285-304 (2009).

58. Janeway, C. A., Travers, P., Walport, M., Shlomchik, M. *Immunobiology: the Immune System in Health and Disease.* Vol. 2 Garland Pub. New York, (2001).

59. Patel, N. S., Lago-Cachón, D., Mohammed, H., Moreno, J. A., Kosel, J. Iron Nanowire Fabrication by Nano-Porous Anodized Aluminum and its Characterization. *Journal of Visualized Experiments.* (152), e60111 (2019).

60. Rao, X. et al. High density gold nanoparticles immobilized on surface via plasma deposited APTES film for decomposing organic compounds in microchannels. *Applied Surface Science.* **439**, 272-281 (2018).

61. Merck. *(3-Aminopropyl)triethoxysilane.* <https://www.sigmaaldrich.com/catalog/product/aldrich/440140?lang=en&region=SA> (2020).

62. Munguía-Cortés, L. et al. APTES-functionalization of SBA-15 using ethanol or toluene: Textural characterization and sorption performance of carbon dioxide. *Journal of the Mexican Chemical Soceity.* **61** (4), 273-281 (2017).

63. Sperling, R. A., Parak, W. J. Surface modification, functionalization and bioconjugation of colloidal inorganic nanoparticles. *Philosophical Transactions of the Royal Society A: Mathematical & Physical Engineering Sciences.* **368** (1915), 1333-1383 (2010).